

Robust spin glass state with exceptional thermal stability in a chemically complex alloy

Jihao Yu ^{1,2} Weiwei Wu ^{1,2} Huaping Zhang,¹ Ruiwen Shao,³ Fan Zhang,⁴ Hong Wang,^{1,2} Zian Li,^{5,*} Junhua Luan,⁶ Zengbao Jiao,⁷ Chain Tsuan Liu ⁶ Baoan Sun ⁶,^{1,2,8,†} Haiyang Bai,^{1,2,8,‡} and Weihua Wang^{1,2,8}

¹*Institute of Physics, Chinese Academy of Sciences, Beijing 100190, China*

²*Center of Materials Science and Optoelectronics Engineering, University of Chinese Academy of Sciences, Beijing 100049, China*

³*Beijing Advanced Innovation Center for Intelligent Robots and Systems, Institute of Engineering Medicine, Beijing Institute of Technology, Beijing 100081, China*

⁴*School of Materials Science and Engineering, Beijing Institute of Technology, Beijing 100081, China*

⁵*School of Physical Science and Technology, Guangxi University, Nanning 530004, China*

⁶*Department of Materials Science and Engineering, City University of Hong Kong, Hong Kong, China*

⁷*Department of Mechanical Engineering, The Hong Kong Polytechnic University, Hong Kong, China*

⁸*Songshan Lake Materials Laboratory, Dongguan, Guangdong 523808, China*



(Received 4 January 2022; revised 29 July 2022; accepted 22 August 2022; published 1 September 2022)

Spin glasses (SGs) arise from the frustration of competing magnetic interactions without long-range order; hence they tend to be destabilized by thermal fluctuation and exhibit a rather low glass transition temperature, presenting a major challenge for SG research and applications. Here, we report an unusual SG state in quaternary Fe-Co-Ni-Mn chemically complex alloys (CCAs). The SG exhibits an ultrahigh freezing temperature above room temperature, well exceeding that of conventional bulk SGs, as well as a unique and fast relaxation dynamics. The thermally stable SG state can be attributed to the strong frustration of exchange interactions owing to the high concentration of magnetic atoms and their chemical randomness in the solid-solution lattice. In addition, owing to the high phase stability of CCAs, the SG is robust over a wide compositional range, enabling a variety of magnetic phase transitions and largely tunable glass properties. These properties make CCAs important for understanding the nature of the SG state and intriguing for practical applications of SGs in spintronics.

DOI: [10.1103/PhysRevMaterials.6.L091401](https://doi.org/10.1103/PhysRevMaterials.6.L091401)

As one of the most intricate magnetic states of matter, spin glass (SG) has stimulated considerable interest in both condensed matter physics and other fields [1–5]. The models and methods developed during the study of SGs over past decades have yielded salient outcomes that are essential for understanding the nature of structural glasses and many other complex systems such as neural networks, optimization algorithms, and protein folding [6–8]. Besides, SG materials themselves are also found to exhibit many novel and exotic physical properties. For example, the random orientation of spins inevitably causes magnetic frustration, which can result in spin chirality and topological magnetic textures [9–11]. Thus they are also intriguing materials for potential applications in spintronic devices [12,13].

Despite years of extensive exploration and studies, the nature of the SG state and the physics underlying the SG transition remain elusive. SGs are formed by freezing the frustrated magnetic moments into one of metastable energy states upon lowering the temperature. For most SG materials, the exchange interactions leading to the frustration are either direct or indirect, i.e., the long-range Ruderman-Kittel-Kasuya-Yosida (RKKY) interaction. Naturally, it is much

weaker in strength than the atomic interaction in structural glasses. Therefore the SG state tends to be overwhelmed by the thermal fluctuation and exhibits a rather low glass transition temperature. So far, there have been a variety of SG materials reported, and the freezing temperatures are found to be in the range 0.135–140 K (Table S1 in the Supplemental Material (SM) [14]). Above the freezing temperature, the non-collinear magnetic structure is suppressed by paramagnetic (PM) or ferromagnetic (FM) orders. Thus the low freezing temperature causes the study of SGs to remain at only a theoretical level, and practical applications can hardly be found. In addition, the key factors governing the freezing temperature of SGs are still poorly understood.

Chemically complex alloys (CCAs) are composed of multiple principal elements, often in near-equiatomic ratios such as high-entropy alloys (HEAs) and medium-entropy alloys (MEAs) [15–19]. The alloying strategy of CCAs stands in stark contrast to the traditional practice that is based mainly on one or two principal elements [20]. As a result, CCAs possess an enormously enlarged compositional space and rich properties to be explored [21,22]. Despite the chemical complexity, CCAs often exhibit a simple solid-solution structure with a high phase stability [22]. These features provide an opportunity to form a SG state if magnetic atoms are introduced into the solid-solution structure. In this Research Letter, we report an unusual SG state in the quaternary Fe-Co-Ni-Mn (FCNM) CCAs, in which Fe, Co, and Ni atoms are FM, while Mn

*zianli@gxu.edu.cn

†sunba@iphy.ac.cn

‡hybai@iphy.ac.cn

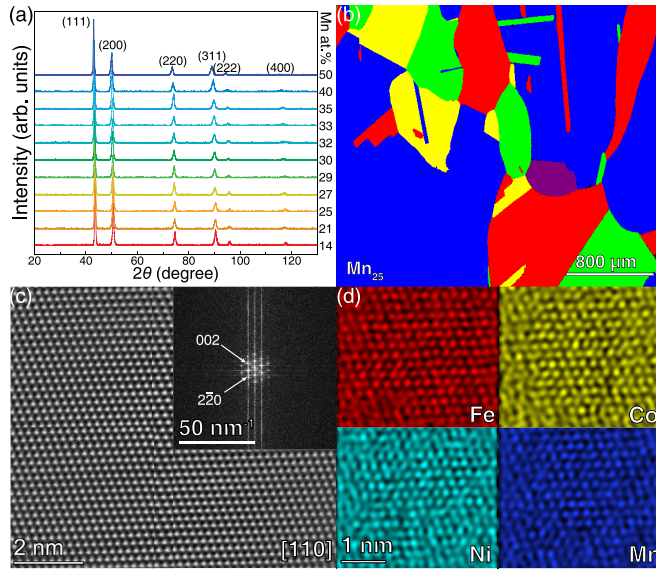


FIG. 1. Structure characterization of FCNM. (a) X-ray diffraction analysis of different samples. All the peaks are well fitted by the fcc structure. (b) EBSD grain map obtained with SEM. (c) HAADF image along the [110] crystal axis and its corresponding FFT pattern (inset). (d) Atomic-resolution EDS mappings acquired from TEM.

atoms are antiferromagnetic (AFM). The interactions among these concentrated magnetic atoms residing on a close-packed lattice result in a strong spin frustration. Consequently, the SG state exhibits a much higher glass transition temperature than that of conventional bulk SG materials and is also robust against large variation of compositions.

CCA samples with nominal compositions of $(\text{FeCoNi})_{100-x}\text{Mn}_x$ ($14 \leq x \leq 50$) (denoted as FCNM alloys) were synthesized by arc-melting pure elements into alloy ingots under an argon atmosphere. The as-cast ingots were further annealed to ensure chemical homogeneities. Details of the sample preparation can be found in the SM [14]. Figure 1(a) shows the x-ray diffraction (XRD) patterns of the samples. The lattice constants calculated from these Bragg peaks are in the range $3.5985\text{--}3.6046$ (± 0.001) Å, which is slightly depending on the content of Mn (see Fig. S1 in the SM [14]). The electron backscattered diffraction (EBSD) grain map of the $(\text{FeCoNi})_{75}\text{Mn}_{25}$ sample (denoted as Mn_{25} hereinafter and similarly for other compositions) in Fig. 1(b) reveals that the alloy is polycrystalline with the grain size reaching the order of millimeters. The EBSD patterns for Mn_{25} can be well fitted by an fcc phase with a lattice constant of 3.6 Å. No other precipitates or phase segregations were observed, proving a single solid-solution phase. The elemental distribution maps obtained by energy-dispersive x-ray spectroscopy (EDS) analyses with scanning electron microscopy (SEM; see Fig. S2 in the SM [14]) show that all four principal elements of Mn_{25} are uniformly distributed at the scale of micrometers. The fluctuation of element density is below 1% (see Fig. S3 as well as Table S2 [14]). According to previous studies, atomic clusters play an important role in the magnetic properties of SGs (such as Au-Fe [23]). There has been short-range order recently reported in medium-entropy alloys [24]. Transmission electron microscopy (TEM)

experiments were performed to check the possible short-range order. Figure 1(c) is the high-angle annular dark-field (HAADF) image of Mn_{25} showing the lattice image of the solid solution along the [110] crystal axis. No extra diffraction information except for the fcc Bragg spot can be found from the fast Fourier transformation (FFT) pattern shown in the inset, confirming the well-defined fcc structure. Selected-area electron diffraction patterns and the HAADF image from the [112] axis can be found in Figs. S4 and S5 in the SM [14], whose results are consistent. The atomic-resolution EDS maps in Cs-corrected TEM [Fig. 1(d)] and corresponding line profiles (see Fig. S6 in the SM [14]) indicate no short- or medium-range order in the alloy. The HAADF images and EDS maps at lower magnifications are shown in Fig. S7 in the SM [14], which also show a uniform distribution of elements. Atom probe tomography (APT; see Fig. S8 in the SM [14]) experiments also demonstrate that no chemical segregations or atomic clusters were detected at nanoscales. Therefore the microstructure of CCAs has been fully characterized at different length scales, from millimeters to subnanometers. These results suggest that FCNM alloys are a single-phase solid solution with no chemical heterogeneities or short- or medium-range orders which have been reported in other CCAs [24].

The temperature-dependent dc $M(T)$ curves for samples with Mn content from 14 to 50% are shown in Figs. 2(a)–2(c). The zero-field-cooled (ZFC) branches and the field-cooled (FC) branches bifurcate at a finite temperature (the bifurcation temperature T_{bf}), which is a typical feature for the formation of a SG state with a broken ergodicity. The magnetic frustration keeps the system from reaching equilibrium within the experimental time scale. It is noted that T_{bf} for Mn_{40} and Mn_{50} samples is even above room temperature (see Fig. S9 in the SM [14]). Although the bifurcation of these $M(T)$ curves is not obvious, the SG nature of high-Mn-content alloys can still be identified by the ac measurements as shown below.

Figure 2(d) shows the real part of ac susceptibility $\chi'(T)$ under various frequencies for the Mn_{25} sample. It exhibits an obvious cusp in 103–109 K depending on the frequency, corresponding to the freezing temperature T_f of the SG state [inset of Fig. 2(d)]. The temperature-dependent heat capacity curve in Fig. S10 in the SM [14] shows no discontinuity or cusp around T_f , which rules out the possibility of FM or AFM transitions. $\chi'(T)$ for Mn_{35} and Mn_{40} are also shown in Fig. S11 in the SM [14] and in Fig. 2(e), respectively. For samples with a higher content of Mn, the net magnetization become weaker because the higher degree of magnetic frustration results in the cancellation of moments and a lower signal-to-noise ratio, making it harder to capture the SG transition especially under moderate fields. Nevertheless, a cusp of $\chi'(T)$ for Mn_{40} and Mn_{50} samples can still be identified at high frequencies, indicating the existence of a SG state. Remarkably, the cusp temperature for Mn_{40} has already been above room temperature (298 K) and even reaches 398 K for Mn_{50} [Fig. 2(f)]. We can see that T_f are ~ 30 K higher than T_{bf} measured under 0.1 T. The relative shift of T_f under different ν (defined as the Mydosh parameter [2] $\delta T_f = \Delta T_f / [T_f \Delta(\log_{10} \nu)]$) is often used to classify distinct SG systems. For Mn_{25} , $\delta T_f = 0.018$ lies between those of dilute magnetic alloys (0.0045 for Au-Mn, 0.005 for Cu-Mn) [2] and

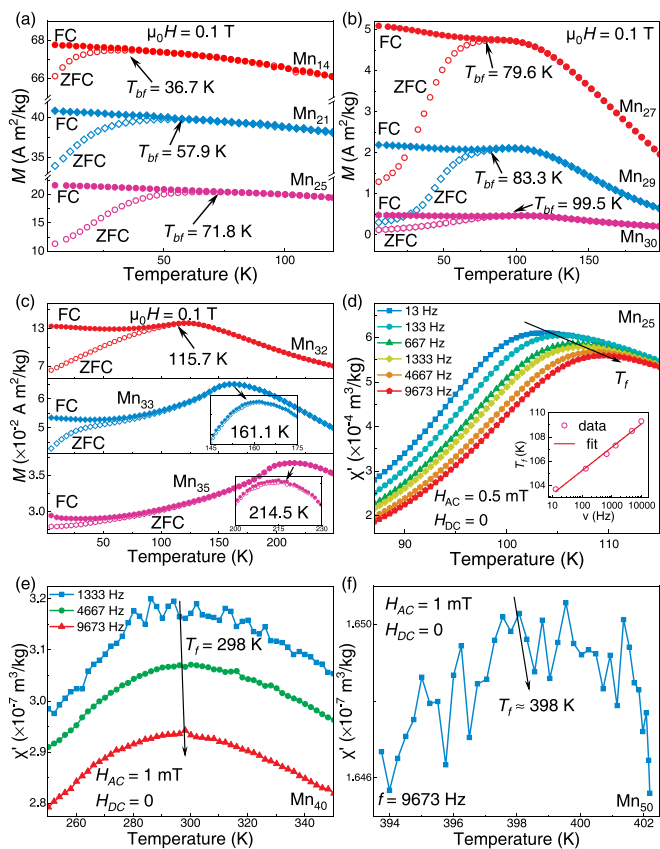


FIG. 2. Magnetic properties of FCNM. (a)–(c) Temperature-dependent dc magnetization of the samples with different compositions. Higher content of Mn induces higher freezing temperature and lower susceptibility. (d)–(f) The real part of ac susceptibility vs temperature for Mn₂₅, Mn₄₀, and Mn₅₀. The inset of (d) shows the freezing temperature T_f as a function of the frequency f .

those of cluster SG systems (0.017 for CrFeGa₂, 0.032 for Nd₅Ge₃) [25,26]. The standard critical-scaling law [27] $\tau = \tau^*(T_f/T_g - 1)^{-z\nu'}$ and the Vogel-Fulcher-Tammann (VFT) law [28] $\tau = \tau_0 \exp[E_a/k_B(T_f - T_0)]$ are employed to analyze the SG dynamics. The results of the fitting parameters (see Fig. S12 in the SM [14]) are comparable to the those reported in other SG systems [29,30]. Among them, the smaller relaxation time of a single spin flip $\tau^* = (4.79 \pm 5.44) \times 10^{-12}$ s and the much larger activation energy $E_a/k_B = 206.6 \pm 5.3$ K as compared with other SG systems suggests a unique and fast relaxation process of the SG state. Magnetic-relaxation and memory-effect experiments for Mn₂₅ (see Fig. S13 in the SM [14]) were also conducted to illustrate the nonequilibrium dynamics. Combining the above experimental evidence, the SG states of the FCNM CCAs can be justified.

We denote the magnetic moment of FC branches at $T = 5$ K under 0.1 T as M_{FC} . Figure 3(a) shows the values of M_{FC} and T_{bf} as functions of Mn content for all FCNM CCAs. One can see that as the Mn content increases from 14% to 35%, M_{FC} decreases drastically by three orders of magnitude and has a negative correlation with T_{bf} . Since the less entangled state is harder to freeze, leading to a lower T_{bf} , and has a more concordant spin configuration that leads to a higher M_{FC} , both T_{bf} and M_{FC} can reflect the degree of magnetic frustration.

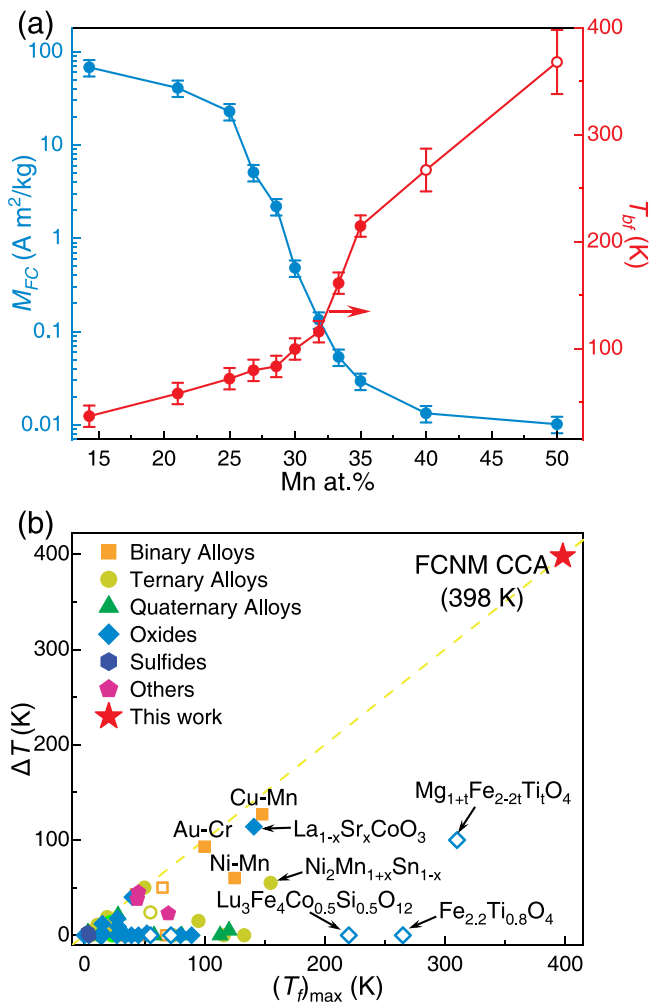


FIG. 3. (a) M_{FC} and T_{bf} obtained from dc magnetization curves. T_{bf} for Mn₄₀ and Mn₅₀ (the red open circles) is derived from ac magnetization data by $T_f - 30$ K. (b) Comparison of glass transition temperature and tunable space between FCNM CCAs and other representative SG systems reported earlier.

Along with the addition of Mn, the FM order is gradually diluted, and its conflict with the AFM one becomes enhanced, resulting in stronger magnetic frustration. The ratio between the Curie temperature T_C (determined by the Curie-Weiss law $\chi = C/(T - T_C)$, where C is a constant; see Fig. S14 in the SM for details [14]) and T_f can also be an index to characterize the degree of frustration [31]. As can be seen in Fig. S15 in the SM [14], both M_{FC} and T_C/T_f show the same trend in the degree of magnetic frustration against the content of Mn.

One striking feature of the SG state observed in FCNM CCAs is the remarkably high T_f , particularly at high Mn contents. T_f for various kinds of SG materials is shown in Table S1 in the SM [14]. The maximum T_f of FCNM CCAs reaches up to 398 K, which is much higher than the highest value of T_f recorded in all SG systems including the bulk and thin-film materials. As far as we know, the T_f for the thin film Mg_{1.5}FeTi_{0.5}O₄ is reported as 310 K owing to the enhanced Dzyaloshinskii-Moriya (DM) interaction induced by the breaking symmetry of interface inversion [32]. Yet the value is still much lower than that of Mn₅₀ we studied here.

The ultrahigh T_f of FCNM CCAs indicates the outstanding thermal stability of the SG state. In addition, T_f can be tuned by continuously varying the composition of FCNM, giving rise to a large ΔT (denoted as the range of T_f that can be reached by tuning the stoichiometry) spanning over 390 K [Fig. 3(b)]. The high T_f and ΔT over a large compositional space enable FCNM CCAs as a model system for studying of SG-related physics and intriguing materials for applications in spintronics. The robustness of the SG state can be ascribed to their stable single-phase fcc structure against composition variation [17,21].

To understand the formation mechanism of SG in FCNM, density functional theory (DFT) calculations have been performed for Mn_{15} , Mn_{25} , and Mn_{35} (see SM for details). Figure 4(a) shows the partial density of states (PDOS) for d orbitals of constituent elements. For Fe, Co, and Ni atoms, the spin-up distribution of the PDOS is more than that of spin-down distribution below the Fermi level, indicating that they behave in a FM-like manner in the alloy. For Mn atoms, the spin peak is above the Fermi level, leading to an AFM behavior. Although the neighboring environments may have altered upon the variation of Mn content, the PDOS remains barely changed, implying that the exchange interaction does not change in type, but only in ratio upon the change in composition. The predicted local magnetic moments of individual atoms at zero temperature (see Fig. S16 in the SM [14]) suggest that Fe, Co, and Ni always behave in a FM-like manner and the spin configurations of Mn are antiparallel in all three systems. The fully relaxed crystal structures and corresponding magnetic moments for each atom are shown in Fig. 4(b). As can be seen, the random alloying gives rise to the geometric frustration of the exchange interactions, which induces the competition between FM and AFM. The FM interactions are predominant at low Mn contents, and the coherence of spins attenuates as the fraction of Mn increases in FCNM alloys. Given that the frustration can result in the SG state, the scenario of magnetic order should be the coexistence of SG with a FM or AFM state in the overall system when either of them takes the prevalence [33,34].

Based on experimental results, we can summarize a magnetic phase diagram for the FCNM CCAs [Fig. 4(c)]. The transition from PM states to FM states can be approximately determined by the downward peaks of the first derivative of the dc magnetization curves, which is common practice for frustrated systems, especially spin glasses [35–39]. The details of determination for each sample can be found in Fig. S18 in the SM [14]. Similarly, the transition into AFM is determined by the Néel temperature T_N . It only appears in the alloys with Mn content above 31%, from which broad peaks in the FC branches of the $M(T)$ curves gradually emerge (Fig. 2). The T_C line meets the T_f line at a critical point. In the composition range $\text{Mn} < 31\%$, the FM order firstly is established from the PM state upon cooling. Furthermore, the spins start to freeze collectively, and the system enters into the SG + FM state. Once the Mn content is above the critical point, the sequential magnetic phase transition changes into $\text{PM} \rightarrow \text{SG} \rightarrow \text{SG} + \text{AFM}$.

For canonical SGs (dilute magnetic alloys), the spin frustrations originate from RKKY interaction which is long ranged and oscillates in sign [2]. Since the interaction is

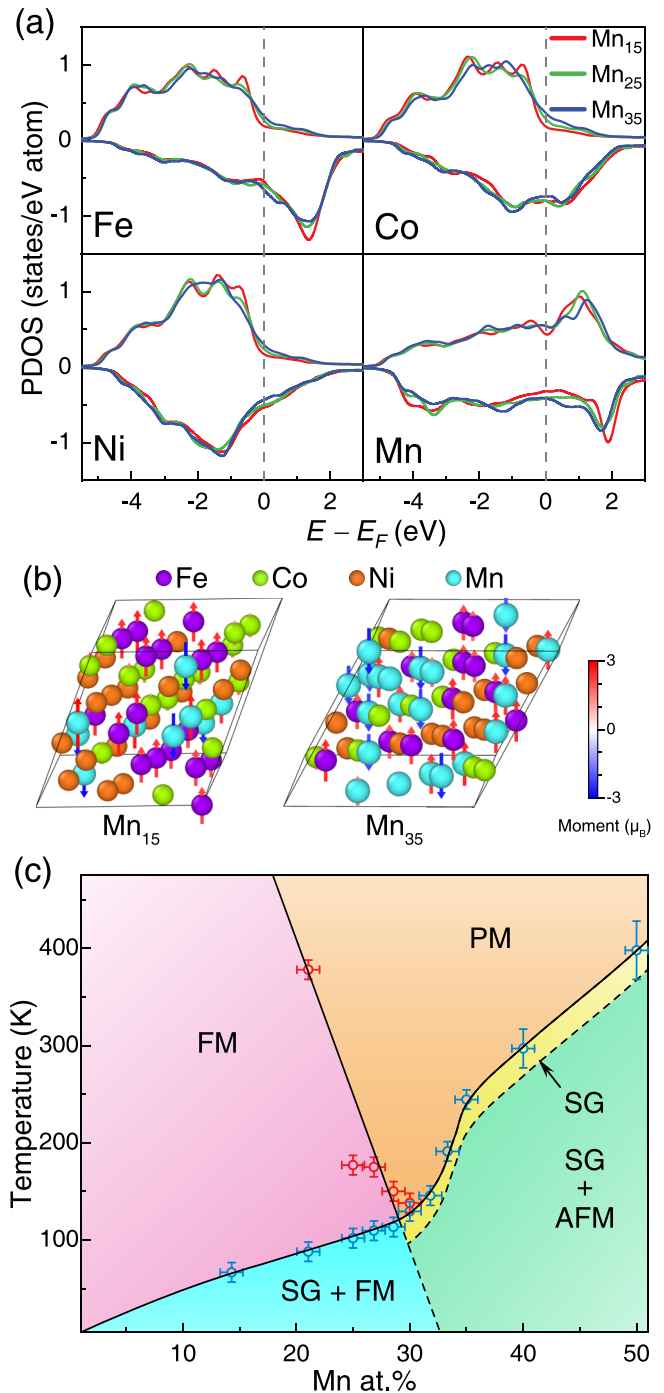


FIG. 4. (a) Partial density of states (PDOS) for d orbitals of Mn, Fe, Co, and Ni in Mn_{15} , Mn_{25} , and Mn_{35} alloys. The energy has been shifted according to the Fermi level. (b) Supercells of Mn_{15} , Mn_{25} , and Mn_{35} for DFT calculation. The length and the colors of the arrows on the atoms indicate the magnetic moments at zero temperature (see Fig. S16 in the SM [14]). Both the atomic coordinates and the lattice parameters are fully relaxed. The final structures remain fcc with slight lattice distortion (see Fig. S17 in the SM [14]). (c) Magnetic phase diagram based on dc and ac magnetization data showing various magnetic orders of FCNM CCAs.

indirect and mediated by conduction electrons, the dilute magnetic $3d$ transition metal atoms yield relatively weak exchange interactions [2]. Therefore canonical SG states are

more susceptible to temperature disorder, manifested as lower T_f . In contrast, for FCNM CCAs, the ordered fcc lattice hosts close-packed magnetic atoms; hence the exchange interaction is direct and short ranged. In addition, the chemical disorder of the elements results in the randomness of both the type and the magnitude of the exchange interaction. These give rise to strong frustrations. For other SG materials in insulating compounds such as $\text{Eu}_x\text{Sr}_{1-x}\text{S}$, their SG behavior comes from the competition of interactions between the nearest neighbors and the next-nearest ones [40]. Without the multiple principal elements, there is no chemical randomness; thus long-range magnetic orders (FM or AFM) are more prone for them to be established. Indeed, their freezing temperatures are generally inferior to canonical SGs as can be seen in Fig. 3(b). Therefore it seems that both the chemical randomness and the short-ranged direct exchange interactions underpin the exceptionally high glass transition temperature.

In conclusion, we report an unusual and robust SG state with a high transition temperature that well exceeds that of all other SG systems. The SG nature has been carefully examined through comprehensive magnetic measurements. The exceptionally high T_f of the SG originates from the strong magnetic frustration, which is closely related to the chemical randomness and short-range exchange interaction. The SG state is also robust against large compositional variation,

which can be ascribed to the stability of the single-phase solid solution. By controlling the proportion of FM and AFM elements without changing the lattice structure, the degree of the magnetic frustration can be precisely regulated, through which novel magnetic structures or spin textures might be developed. This mechanism also paves an avenue for designing strongly magnetically frustrated systems. Finally, it is worth noting that the CCAs can be easily cast into the bulk and plastically processed as compared with other SG materials. The strikingly high T_f and the large tunability, in combination with the high processability, enable FCNM CCAs to be model systems for studying SG physics and attractive materials in spintronic applications.

This research was supported by the National Key Research and Development Plan (Grant No. 2018YFA0703603), Guangdong Major Project of Basic and Applied Basic Research, China (Grant No. 2019B030302010), National Natural Science Foundation of China (Grants No. 52192602, No. 51822107, No. 61888102, No. 11790291, and No. 11974019), and Strategic Priority Research Program of the Chinese Academy of Sciences (XDB30000000). Atom probe tomography research was conducted at the Inter-University 3D Atom Probe Tomography Unit of City University of Hong Kong, which is supported by CityU Grant No. 9360161.

-
- [1] K. Binder and A. P. Young, *Rev. Mod. Phys.* **58**, 801 (1986).
- [2] J. A. Mydosh, *Spin Glasses: An Experimental Introduction* (Taylor & Francis, London, 1993).
- [3] G. Parisi, *Proc. Natl. Acad. Sci. USA* **103**, 7948 (2006).
- [4] J. A. Mydosh, *Rep. Prog. Phys.* **78**, 052501 (2015).
- [5] H. Kawamura and T. Taniguchi, in *Handbook of Magnetic Materials*, Vol. 24 (Elsevier, New York, 2015), pp. 1–137.
- [6] L. Personnaz, I. Guyon, and G. Dreyfus, *J. Phys. Lett.* **46**, 359 (1985).
- [7] N. Sourlas, *Nature (London)* **339**, 693 (1989).
- [8] R. A. Goldstein, Z. A. Luthey-Schulten, and P. G. Wolynes, *Proc. Natl. Acad. Sci. USA* **89**, 4918 (1992).
- [9] H. Kawamura, *Phys. Rev. Lett.* **90**, 047202 (2003).
- [10] T. Taniguchi, K. Yamanaka, H. Sumioka, T. Yamazaki, Y. Tabata, and S. Kawarazaki, *Phys. Rev. Lett.* **93**, 246605 (2004).
- [11] B. Pang, L. Zhang, Y. B. Chen, J. Zhou, S. Yao, S. Zhang, and Y. Chen, *ACS Appl. Mater. Interfaces* **9**, 3201 (2017).
- [12] Y. Li, L. Zhang, Q. Zhang, C. Li, T. Yang, Y. Deng, L. Gu, and D. Wu, *ACS Appl. Mater. Interfaces* **11**, 21268 (2019).
- [13] E. Maniv, N. L. Nair, S. C. Haley, S. Doyle, C. John, S. Cabrini, A. Maniv, S. K. Ramakrishna, Y.-L. Tang, P. Ercius, R. Ramesh, Y. Tserkovnyak, A. P. Reyes, and J. G. Analytis, *Sci. Adv.* **7**, eabd8452 (2021).
- [14] See Supplemental Material at <http://link.aps.org/supplemental/10.1103/PhysRevMaterials.6.L091401> for details on materials and methods, Figs. S1–S10, and Tables S1 and S2, which includes Refs. [23,25,26,29,30,32,35,40–112].
- [15] J. W. Yeh, S. K. Chen, S. J. Lin, J. Y. Gan, T. S. Chin, T. T. Shun, C. H. Tsau, and S. Y. Chang, *Adv. Eng. Mater.* **6**, 299 (2004).
- [16] B. Gludovatz, A. Hohenwarter, D. Catoor, E. H. Chang, E. P. George, and R. O. Ritchie, *Science* **345**, 1153 (2014).
- [17] M.-H. Tsai and J.-W. Yeh, *Mater. Res. Lett.* **2**, 107 (2014).
- [18] Z. Li, K. G. Pradeep, Y. Deng, D. Raabe, and C. C. Tasan, *Nature (London)* **534**, 227 (2016).
- [19] E. P. George, D. Raabe, and R. O. Ritchie, *Nat. Rev. Mater.* **4**, 515 (2019).
- [20] D. B. Miracle and O. N. Senkov, *Acta Mater.* **122**, 448 (2017).
- [21] Y. Zhang, T. T. Zuo, Z. Tang, M. C. Gao, K. A. Dahmen, P. K. Liaw, and Z. P. Lu, *Prog. Mater. Sci.* **61**, 1 (2014).
- [22] W. Li, D. Xie, D. Li, Y. Zhang, Y. Gao, and P. K. Liaw, *Prog. Mater. Sci.* **118**, 100777 (2021).
- [23] B. R. Coles, B. V. B. Sarkissian, and R. H. Taylor, *Philos. Mag. B* **37**, 489 (1978).
- [24] X. Chen, Q. Wang, Z. Cheng, M. Zhu, H. Zhou, P. Jiang, L. Zhou, Q. Xue, F. Yuan, J. Zhu, X. Wu, and E. Ma, *Nature (London)* **592**, 712 (2021).
- [25] B. Maji, K. G. Suresh, and A. K. Nigam, *J. Phys.: Condens. Matter* **23**, 506002 (2011).
- [26] P. Bag, P. R. Baral, and R. Nath, *Phys. Rev. B* **98**, 144436 (2018).
- [27] P. C. Hohenberg and B. I. Halperin, *Rev. Mod. Phys.* **49**, 435 (1977).
- [28] J. Souletie and J. L. Tholence, *Phys. Rev. B* **32**, 516 (1985).
- [29] J. Kroder, J. Gooth, W. Schnelle, G. H. Fecher, and C. Felser, *AIP Adv.* **9**, 055327 (2019).
- [30] P. Bag, K. Somesh, and R. Nath, *J. Magn. Magn. Mater.* **497**, 165977 (2020).

- [31] H. Luo, J. W. Krizan, E. M. Seibel, W. Xie, G. S. Sahasrabudhe, S. L. Bergman, B. F. Phelan, J. Tao, Z. Wang, J. Zhang, and R. J. Cava, *Chem. Mater.* **27**, 6810 (2015).
- [32] Y. Muraoka, H. Tabata, and T. Kawai, *Appl. Phys. Lett.* **76**, 1179 (2000).
- [33] K. Westerholt and H. Bach, *Phys. Rev. B* **31**, 7151 (1985).
- [34] A. D. Beath and D. H. Ryan, *Phys. Rev. B* **76**, 064410 (2007).
- [35] L. Xue, L. Shao, Q. Luo, and B. Shen, *J. Alloys Compd.* **790**, 633 (2019).
- [36] S. Gondh, M. M. Patidar, K. Kumar, M. P. Saravanan, V. Ganesan, and A. K. Pramanik, *Phys. Rev. B* **104**, 014401 (2021).
- [37] V. A. Turchenko, S. V. Trukhanov, V. G. Kostishin, F. Damay, F. Porcher, D. S. Klygach, M. G. Vakhtov, D. Lyakhov, D. Michels, B. Bozzo, I. Fina, M. A. Almessiere, Y. Slimani, A. Baykal, D. Zhou, and A. V. Trukhanov, *Sci. Rep.* **11**, 18342 (2021).
- [38] A. K. Singh and R. Chandra, *J. Magn. Magn. Mater.* **549**, 169048 (2022).
- [39] D. Kumar and A. K. Singh, *J. Solid State Chem.* **309**, 122986 (2022).
- [40] H. Maletta, *J. Appl. Phys.* **53**, 2185 (1982).
- [41] A. Zunger, S.-H. Wei, L. G. Ferreira, and J. E. Bernard, *Phys. Rev. Lett.* **65**, 353 (1990).
- [42] A. van de Walle, *Calphad* **33**, 266 (2009).
- [43] A. van de Walle, P. Tiwary, M. de Jong, D. Olmsted, M. Asta, A. Dick, D. Shin, Y. Wang, L.-Q. Chen, and Z.-K. Liu, *Calphad* **42**, 13 (2013).
- [44] G. Kresse and D. Joubert, *Phys. Rev. B* **59**, 1758 (1999).
- [45] J. P. Perdew, K. Burke, and M. Ernzerhof, *Phys. Rev. Lett.* **77**, 3865 (1996).
- [46] M. Methfessel and A. T. Paxton, *Phys. Rev. B* **40**, 3616 (1989).
- [47] H. J. Monkhorst and J. D. Pack, *Phys. Rev. B* **13**, 5188 (1976).
- [48] R. V. Chamberlin, *J. Appl. Phys.* **57**, 3377 (1985).
- [49] J. Kroder, K. Manna, D. Kriegner, A. S. Sukhanov, E. Liu, H. Borrmann, A. Hoser, J. Gooth, W. Schnelle, D. S. Inosov, G. H. Fecher, and C. Felser, *Phys. Rev. B* **99**, 174410 (2019).
- [50] F. Lefloch, J. Hammann, M. Ocio, and E. Vincent, *Europhys. Lett.* **18**, 647 (1992).
- [51] Y. Nakai, M. Sakuma, and N. Kunitomi, *J. Phys. Soc. Jpn.* **56**, 301 (1987).
- [52] S. Sharma, E. P. Amaladass, and A. Mani, *Mater. Des.* **131**, 204 (2017).
- [53] N. B. Brandt and V. V. Moshchalkov, *Adv. Phys.* **33**, 193 (1984).
- [54] A. Mauger, J. Ferré, M. Ayadi, and P. Nordblad, *Phys. Rev. B* **37**, 9022 (1988).
- [55] A. Haldar, K. G. Suresh, and A. K. Nigam, *Europhys. Lett.* **91**, 67006 (2010).
- [56] C. Tien, J. J. Lu, and L. Y. Jang, *Phys. Rev. B* **65**, 214416 (2002).
- [57] J. M. Rojo, J. L. Mesa, L. Lezama, J. L. Pizarro, M. I. Arriortua, J. R. Fernandez, G. E. Barberis, and T. Rojo, *Phys. Rev. B* **66**, 094406 (2002).
- [58] S. Thota and M. S. Seehra, *J. Appl. Phys.* **113**, 203905 (2013).
- [59] Y. Iijima, Y. Kamei, N. Kobayashi, J. Awaka, T. Iwasa, S. Ebisu, S. Chikazawa, and S. Nagata, *Philos. Mag.* **83**, 2521 (2003).
- [60] P. Gibbs, T. M. Harders, and J. H. Smith, *J. Phys. F: Met. Phys.* **15**, 213 (1985).
- [61] P. R. T. Ribeiro, F. L. A. Machado, D. C. Harrison, E. Dan Dahlberg, and S. M. Rezende, *J. Magn. Magn. Mater.* **541**, 168537 (2022).
- [62] S. Zapf, H. S. Jeevan, T. Ivek, F. Pfister, F. Klingert, S. Jiang, D. Wu, P. Gegenwart, R. K. Kremer, and M. Dressel, *Phys. Rev. Lett.* **110**, 237002 (2013).
- [63] M. D. Mukadam, S. M. Yusuf, P. Sharma, S. K. Kulshreshtha, and G. K. Dey, *Phys. Rev. B* **72**, 174408 (2005).
- [64] G. Aeppli, S. M. Shapiro, R. J. Birgeneau, and H. S. Chen, *Phys. Rev. B* **28**, 5160 (1983).
- [65] K. Jonason, J. Mattsson, and P. Nordblad, *Phys. Rev. B* **53**, 6507 (1996).
- [66] H. Yamahara, M. Seki, M. Adachi, M. Takahashi, H. Nasu, K. Horiba, H. Kumigashira, and H. Tabata, *J. Appl. Phys.* **118**, 063905 (2015).
- [67] H. Shiraiishi, M. Sugamura, and T. Hori, *J. Magn. Magn. Mater.* **70**, 230 (1987).
- [68] T. Samanta, P. A. Bhowe, A. Das, A. Kumar, and A. K. Nigam, *Phys. Rev. B* **97**, 184421 (2018).
- [69] P. Schiffer, A. P. Ramirez, D. A. Huse, P. L. Gammel, U. Yaron, D. J. Bishop, and A. J. Valentino, *Phys. Rev. Lett.* **74**, 2379 (1995).
- [70] S. H. Song, M. H. Jung, and S. H. Lim, *J. Phys.: Condens. Matter* **19**, 036211 (2007).
- [71] J. Dho, W. S. Kim, and N. H. Hur, *Phys. Rev. Lett.* **89**, 027202 (2002).
- [72] P. A. Kumar, R. Mathieu, P. Nordblad, S. Ray, O. Karis, G. Andersson, and D. D. Sarma, *Phys. Rev. X* **4**, 011037 (2014).
- [73] A. Malinowski, V. L. Bezusyy, R. Minikayev, P. Dziawa, Y. Syryanyy, and M. Sawicki, *Phys. Rev. B* **84**, 024409 (2011).
- [74] J. Wu and C. Leighton, *Phys. Rev. B* **67**, 174408 (2003).
- [75] J. Krishna Murthy and A. Venimadhav, *J. Appl. Phys.* **113**, 163906 (2013).
- [76] J. Pérez, J. García, J. Blasco, and J. Stankiewicz, *Phys. Rev. Lett.* **80**, 2401 (1998).
- [77] M. Viswanathan and P. S. A. Kumar, *Phys. Rev. B* **80**, 012410 (2009).
- [78] M. Tachibana, T. Tojo, H. Kawaji, T. Atake, H. Ikuta, Y. Uchimoto, and M. Wakihara, *Phys. Rev. B* **66**, 092406 (2002).
- [79] X. Bie, Y. Gao, X. Yang, Y. Wei, H. Ehrenberg, M. Hinterstein, G. Chen, C. Wang, and F. Du, *J. Alloys Compd.* **626**, 150 (2015).
- [80] H. Yamahara, M. Seki, and H. Tabata, *J. Magn. Magn. Mater.* **501**, 166437 (2020).
- [81] Y. Muraoka, H. Tabata, and T. Kawai, *Appl. Phys. Lett.* **77**, 4016 (2000).
- [82] H. Zeng, G. Yu, Y. Yuan, W. Wang, X. Luo, C. Chen, S. Ur Rehman, G. Yuan, S. Ma, and Z. Zhong, *J. Magn. Magn. Mater.* **521**, 167532 (2021).
- [83] W. J. Feng, D. Li, W. J. Ren, Y. B. Li, W. F. Li, J. Li, Y. Q. Zhang, and Z. D. Zhang, *Phys. Rev. B* **73**, 205105 (2006).
- [84] X. H. Zhang, Q. Yuan, J. C. Han, J. G. Zhao, J. K. Jian, Z. H. Zhang, and B. Song, *Appl. Phys. Lett.* **103**, 022405 (2013).
- [85] B. Song, J. Jian, H. Bao, M. Lei, H. Li, G. Wang, Y. Xu, and X. Chen, *Appl. Phys. Lett.* **92**, 192511 (2008).
- [86] Q. Zhang, D. Li, W. B. Cui, J. Li, and Z. D. Zhang, *J. Appl. Phys.* **106**, 113915 (2009).
- [87] T. Gao, K. Nishimura, T. Namiki, and H. Okimoto, *J. Appl. Phys.* **111**, 013913 (2012).

- [88] D. X. Li, S. Nimori, Y. Shiokawa, A. Tobo, H. Onodera, Y. Haga, E. Yamamoto, and Y. nuki, *Appl. Phys. Lett.* **79**, 4183 (2001).
- [89] J. Blasco and J. García, *Phys. Rev. B* **51**, 3569 (1995).
- [90] A. K. Singh, S. Chauhan, and R. Chandra, *Appl. Phys. Lett.* **110**, 102402 (2017).
- [91] P. Liao, C. Jing, X. L. Wang, Y. J. Yang, D. Zheng, Z. Li, B. J. Kang, D. M. Deng, S. X. Cao, J. C. Zhang, and B. Lu, *Appl. Phys. Lett.* **104**, 092410 (2014).
- [92] A. K. Nayak, K. G. Suresh, and A. K. Nigam, *J. Phys.: Condens. Matter* **23**, 416004 (2011).
- [93] S. Chatterjee, S. Giri, S. K. De, and S. Majumdar, *Phys. Rev. B* **79**, 092410 (2009).
- [94] M. K. Ray, K. Bagani, P. K. Mukhopadhyay, and S. Banerjee, *Europhys. Lett.* **109**, 47006 (2015).
- [95] Y. J. Zhang, Q. Q. Zeng, Z. Y. Wei, Z. P. Hou, Z. H. Liu, E. K. Liu, X. K. Xi, W. H. Wang, X. Q. Ma, and G. H. Wu, *J. Alloys Compd.* **749**, 134 (2018).
- [96] W. Abdul-Razzaq and J. S. Kouvel, *J. Appl. Phys.* **55**, 1623 (1984).
- [97] S. C. Ho, I. Maartense, and G. Williams, *J. Appl. Phys.* **53**, 2235 (1982).
- [98] E. A. Goremychkin, R. Osborn, B. D. Rainford, R. T. Macaluso, D. T. Adroja, and M. Koza, *Nat. Phys.* **4**, 766 (2008).
- [99] M. Svedberg, S. Majumdar, H. Huhtinen, P. Paturi, and S. Granroth, *J. Phys.: Condens. Matter* **23**, 386005 (2011).
- [100] V. K. Anand, D. T. Adroja, and A. D. Hillier, *Phys. Rev. B* **85**, 014418 (2012).
- [101] S. Pakhira, C. Mazumdar, R. Ranganathan, and S. Giri, *J. Alloys Compd.* **742**, 391 (2018).
- [102] T. Scholz and R. Dronskowski, *AIP Adv.* **6**, 055107 (2016).
- [103] B. S. Wang, P. Tong, Y. P. Sun, X. B. Zhu, Z. R. Yang, W. H. Song, and J. M. Dai, *Appl. Phys. Lett.* **97**, 042508 (2010).
- [104] A. Poddar and C. Mazumdar, *J. Appl. Phys.* **106**, 093908 (2009).
- [105] B. Yuan, J. Yang, X. Z. Zuo, D. P. Song, X. W. Tang, X. B. Zhu, J. M. Dai, W. H. Song, and Y. P. Sun, *J. Appl. Phys.* **117**, 233906 (2015).
- [106] J. J. Hauser, *Phys. Rev. B* **34**, 3212 (1986).
- [107] D. X. Li, T. Yamamura, S. Nimori, K. Yubuta, and Y. Shiokawa, *Appl. Phys. Lett.* **87**, 142505 (2005).
- [108] D. Kaczorowski and H. Noel, *J. Phys.: Condens. Matter* **5**, 9185 (1993).
- [109] D. X. Li, S. Nimori, T. Yamamura, and Y. Shiokawa, *J. Appl. Phys.* **103**, 07B715 (2008).
- [110] D. X. Li, Y. Shiokawa, Y. Homma, A. Uesawa, A. Dönni, T. Suzuki, Y. Haga, E. Yamamoto, T. Honma, and Y. Ōnuki, *Phys. Rev. B* **57**, 7434 (1998).
- [111] Q.-Q. Gao, J.-B. Li, G.-N. Li, G.-H. Rao, J. Luo, G.-Y. Liu, and J.-K. Liang, *J. Appl. Phys.* **114**, 053901 (2013).
- [112] T. Chakrabarty, A. V. Mahajan, and S. Kundu, *J. Phys.: Condens. Matter* **26**, 405601 (2014).